Available online at www.sciencedirect.com
ScienceDirect
Energy Reports 8 (2022) 832–842
www.elsevier.com/locate/egyr

The 5th International Conference on Electrical Engineering and Green Energy, CEEGE 2022, 8–11 June, Berlin, Germany

Optimal location and capacity planning of UPQCs considering operation dispatching in distribution grid with distributed generators

Xiaoguang Zhu[a], Yubo Guo[a], Shurong Li[a], Junbo Deng[a,*], Tenghao Ji[b]

[a] *Xi'an Jiaotong University, Xi'an 710049, China*
[b] *The Hong Kong Polytechnic University, Hong Kong, China*

Received 25 July 2022; accepted 6 August 2022
Available online 23 August 2022

Abstract

The unified power quality conditioner (UPQC) has prospects in power quality management considering green energy integration. This paper proposes an optimization method for the location and capacity planning of UPQCs in the distribution grid with distributed generators. The planning and dispatching of UPQCs are combined into a coupled optimization model in this paper. The dual-controlled-source model is proposed and well used to describe the operation state of UPQC. Fluctuations in the output of wind generators and photovoltaic power plants are also taken into account. The improved golden eagle optimization (IMOGEO) algorithm, based on the two-archive strategy, can better balance the convergence and diversity of the non-dominated solution set. A case study is carried out based on the modified IEEE 33-node distribution grid model including DGs and loads with a diurnal variation. The optimized schemes of location and capacity are obtained, and the corresponding dispatching strategies display the superiority in both voltage variation and line loss. The results verify the effectiveness and advantages of the proposed method.

Peer-review under responsibility of the scientific committee of the 5th International Conference on Electrical Engineering and Green Energy, CEEGE, 2022.

Keywords: UPQC; Location and capacity planning; Optimal dispatching; Distributed generator; Power quality management

1. Introduction

A high proportion of new energy is becoming an inevitable development trend of the future power system. With the large-scale integration of renewable energy, power quality regulation and reactive power compensation devices have increasingly become an important part of the distribution grid [1]. Unified power quality conditioner (UPQC), as a powerful flexible AC transmission system (FACTS) equipment, can reduce the active power loss in the transmission lines and improve power transmission capacity by adopting appropriate control methods. The output reactive current of UPQC does not depend on the system voltage, which can greatly improve the dynamic stability of the load voltage. However, if the installation location of the UPQC is not properly selected, it may

* Corresponding author.
E-mail address: dengjb@mail.xjtu.edu.cn (J. Deng).

https://doi.org/10.1016/j.egyr.2022.08.133

Peer-review under responsibility of the scientific committee of the 5th International Conference on Electrical Engineering and Green Energy, CEEGE, 2022.

lead to problems such as increased energy loss and poor stability. At the same time, improper selection of capacity will result in a waste of investment costs. Therefore, it is very important to choose the installation location and capacity of UPQC reasonably. Placement selection, capacity planning, and operation dispatching constitute a set of interrelated optimal power flow problems for UPQCs. This optimization problem is discontinuous, nonlinear, and high-dimensional, which makes it difficult to solve.

In recent years, some meta-heuristic intelligent optimization algorithms have been used to solve the optimal power flow problem related to UPQC. Dr. Ganguly [2] obtained a non-dominated solution set for UPQC location and capacity using multi-objective particle swarm optimization (MOPSO). A power flow algorithm including the UPQC-PAC model is proposed and applied. Sarker and Goswami [3] introduced the optimal allocation of UPQC based on the cuckoo optimization algorithm (COA) in a three-phase unbalanced distribution grid. Han et al. [4] transformed the multi-objective optimization problem of UPQC into several single-objective optimization problems. By solving the single-objective optimization problem, the operation of UPQC is divided into four simple optimal operation modes. Amini and Jalilian [5] studied the optimal configuration of an open unified power quality conditioner (OUPQC) in smart distribution grids, and this paper takes into account the utilization and load growth of OUPQC. In these studies, the optimization goal of UPQC focused on location and capacity planning, while the optimization of operation dispatching is often ignored. They assume that UPQC works in some specified operating mode. Moreover, previous studies did not take into account the impact of the grid connection of renewable energy and its output volatility on the operation of UPQC.

Therefore, considering the incorporation of renewable energy, this paper combines the optimal planning and optimal dispatching problems of UPQCs to establish a coupled optimization model. A new intelligent optimization algorithm is introduced into the solution process of this optimization problem. Mohammadi-Balani et al. [6] proposed the golden eagle optimizer (GEO), which is a meta-heuristic algorithm based on the simulation of golden eagle hunting behavior. It shows superior performance in solving multi-objective optimization problems. However, the multi-objective golden eagle optimization (MOGEO) algorithm tends to fall into local optimum when solving high-dimensional optimization problems. Thus, this paper makes substantial improvements to the algorithm so that it can be used to solve the optimal power flow problem.

2. Dual-controlled-source model of UPQC

UPQC is a powerful FACTS device used to improve power quality issues such as voltage fluctuations and current harmonics in power supplies. However, UPQC operates in reactive power compensation mode for most of the time since the voltage fluctuation occurs and lasts only for a short time. For sparse distribution grids in remote areas, UPQC is also used to manage the voltage sag problem of long-distance distribution lines. Therefore, reactive power compensation and voltage sag suppression are the main concerns of this paper. Fig. 1 shows a typical structure of UPQC. It consists of a shunt converter, a shunt transformer, a series converter, a series transformer, and a DC capacitor. It also includes voltage and current signal detection, control, and pulse modulation devices. The shunt unit of this UPQC is close to the power supply side, so it is also called UPQC-L. UPQC with this structure is well suitable for reactive power compensation and voltage sag suppression.

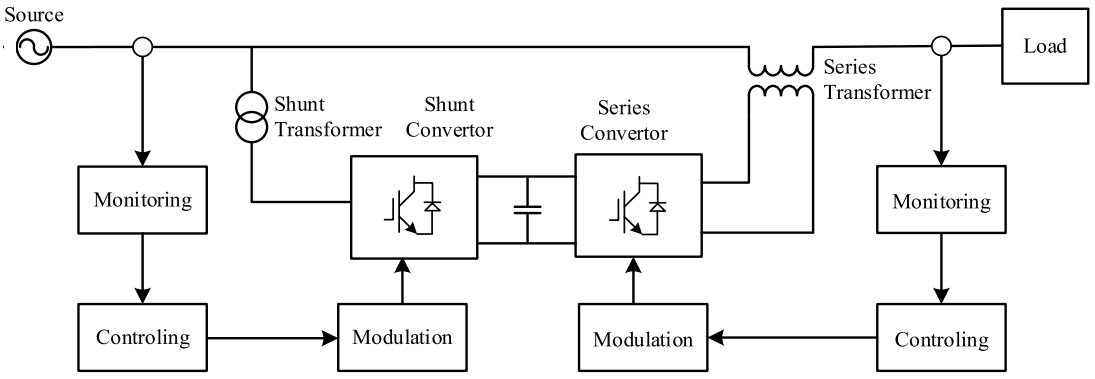

Fig. 1. A typical topology of UPQC.

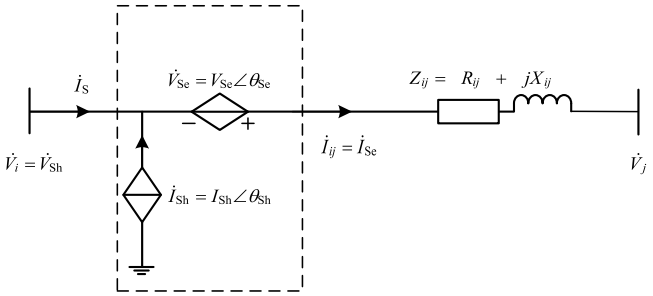

Fig. 2. Dual-controlled-source model of UPQC in single-phase equivalent circuit of distribution lines.

Aiming at compensating the reactive power and suppressing the voltage sag in distribution lines, this paper proposes an equivalent model of UPQC under steady-state operation. As shown in Fig. 2, UPQC is equivalent to a dual-controlled-source (DCS) model, i.e., a combination of a shunt controlled current source and a series controlled voltage source. The amplitude V_{Se} and phase θ_{Se} of the series controlled voltage source, and the amplitude I_{Sh} and the phase θ_{Sh} of the shunt controlled current source, jointly determine the operating state of the UPQC. That is to say, the operation control instruction of UPQC at any time can be given by the column vector $\boldsymbol{I}$= $[I_{Sh}, \theta_{Sh}, V_{Se}, \theta_{Se}]^T$, and the corresponding power state variables are

$$\begin{cases} \dot{S}_{Sh} = \dot{V}_{Sh}\dot{I}_{Sh}^* = P_{Sh} + jQ_{Sh} \\ P_{Sh} = \mathrm{Re}\left(\dot{V}_{Sh}\dot{I}_{Sh}^*\right) \\ Q_{Sh} = \mathrm{Im}\left(\dot{V}_{Sh}\dot{I}_{Sh}^*\right) \\ \dot{S}_{Se} = \dot{V}_{Se}\dot{I}_{Se}^* = P_{Se} + jQ_{Se} \\ P_{Se} = \mathrm{Re}\left(\dot{V}_{Se}\dot{I}_{Se}^*\right) \\ Q_{Se} = \mathrm{Im}\left(\dot{V}_{Se}\dot{I}_{Se}^*\right) \end{cases} \tag{1}$$

where P_{Sh}, Q_{Sh}, and $\dot{S}_{Sh}$ are respectively active power, reactive power, and complex power emitted by the shunt controlled current source; P_{Se}, Q_{Se}, and $\dot{S}_{Se}$ are respectively active power, reactive power, and complex power emitted by the series controlled voltage source; $\dot{V}_{Se}$, $\dot{I}_{Se}$, $\dot{V}_{Sh}$, and $\dot{I}_{Sh}$ are the voltage and current phasors of the series controlled voltage source and the parallel controlled current source, respectively.

Assuming that the UPQC has no active power loss in steady-state operation, the algebraic sum of the active power emitted by the series part and the shunt part is zero, i.e.

$$\mathrm{Re}\left(\dot{V}_{Sh}\dot{I}_{Sh}^*\right) + \mathrm{Re}\left(\dot{V}_{Se}\dot{I}_{Se}^*\right) = 0 \tag{2}$$

Under the constraint of (2), the operation control instructions of the dual-controlled-source model reduce one degree of freedom, namely

$$\theta_{Sh} = \arccos\frac{-V_{Se}\left|\dot{I}_{Se}\right|\cos(\theta_{Se} - \theta_{I_{Se}})}{I_{Sh}\left|\dot{V}_{Sh}\right|} + \theta_{V_{Sh}} \tag{3}$$

where $\theta_{I_{Se}}$ and $\theta_{V_{Sh}}$ are the phases of $\dot{I}_{Se}$ and $\dot{V}_{Sh}$, respectively.

Therefore, the operation control instructions of UPQC have 3 degrees of freedom, which is denoted as

$$\boldsymbol{I} = [I_{Sh}, V_{Se}, \theta_{Se}]^T \tag{4}$$

All feasible instructions satisfying (4) form a three-dimensional instruction space. When UPQC adopts a specific control mode, such as UPQC-P, UPQC-Q, or UPQC-VA, the instruction space will be further reduced in dimension. In UPQC-P mode, for example, the series equivalent controlled voltage source is kept in the same phase with the current flowing through it, i.e., $\theta_{Se} = \theta_{I_{Se}}$. At this time, the dimension of the control instruction in Eq. (4) will be reduced to 2. It is worth noting that this paper pursues the maximization of the feasible range when considering the optimal problem of distribution grid power flow. Therefore, until the optimal instruction is found, no specific control

mode will be adopted for the UPQC. In other words, this paper adopts the three-dimensional control instruction shown in formula (4).

3. Optimization model for location and capacity of UPQCs considering operation dispatching

For simplicity, the following assumptions are made for the distribution grid with distributed generators and UPQCs: (a) Distributed generators do not emit or absorb reactive power. (b) Similarly, the active power consumption of UPQCs is not considered, that is, they neither emit nor absorb active power externally. (c) Each device is connected to the network branch and closer to the power sending terminal rather than the receiving terminal.

In the optimization of location and capacity planning the decision variables are defined as the installation location, shunt capacity, and series capacity of UPQC. For another, in the optimization of operation dispatching, the decision variables are defined as in (4). The two optimization problems are nested with each other and can be integrated into a coupled optimization model. Therefore, the decision variables are defined as

$$\boldsymbol{X} = [\boldsymbol{L}, \overline{\boldsymbol{S}}_{\mathrm{Sh}}, \overline{\boldsymbol{S}}_{\mathrm{Se}}, \boldsymbol{I}_{\mathrm{Sh}}, \boldsymbol{V}_{\mathrm{Se}}, \boldsymbol{\theta}_{\mathrm{Se}}]^{\mathrm{T}} \tag{5}$$

where the vector $\boldsymbol{L}$ represents the installation location of the UPQCs, and their shunt capacity and series capacity are represented by vectors $\overline{\boldsymbol{S}}_{\mathrm{Sh}}$ and $\overline{\boldsymbol{S}}_{\mathrm{Se}}$, respectively; $\boldsymbol{I}_{\mathrm{Sh}}$ is the amplitude of UPQC shunt current; $\boldsymbol{V}_{\mathrm{Se}}$ is the amplitude of UPQC series voltage; θ_{Se} is the phase of UPQC series voltage. Each variable in the above formula is time-varying.

The coupled optimization model can be expressed as

$$\min \boldsymbol{f} = [f_{\mathrm{Cost}}, f_{\mathrm{Volt}}, f_{\mathrm{Loss}}]^{\mathrm{T}} \tag{6}$$

$$\text{where } f_{\mathrm{Cost}} = \boldsymbol{C}_{\mathrm{U}}^{\mathrm{T}} \left(\overline{\boldsymbol{S}}_{\mathrm{Se}} + \overline{\boldsymbol{S}}_{\mathrm{Sh}}\right) \cdot (1 + \lambda_{\mathrm{U}}) \tag{7}$$

$$f_{\mathrm{Volt}} = \frac{1}{T\Delta t} \sum_{t=\Delta t}^{T\Delta t} \sqrt{\frac{1}{N} \sum_{i=1}^{N} \left(U_{i,t} - 1\right)^2} \tag{8}$$

$$f_{\mathrm{Loss}} = \frac{1}{T\Delta t} \sum_{t=\Delta t}^{T\Delta t} \sum_{i,j \in N_L} G_{ij} \left(U_{i,t}^2 + U_{j,t}^2 - 2U_{i,t}U_{j,t}\cos\theta_{ij,t}\right) \Delta t \tag{9}$$

$$\text{s.t.} \quad 0 \le N_{\mathrm{U}} = Dim(\boldsymbol{L}) \le N_{\mathrm{B}}, \boldsymbol{L}(i) \in \{1, 2, \ldots, N_{\mathrm{B}}\}, \quad \boldsymbol{L}(i) \ne \boldsymbol{L}(j), \quad i, j \in \{1, 2, \ldots, N_{\mathrm{U}}\}, i \ne j \tag{10}$$

$$P_{\mathrm{WG},i} + P_{\mathrm{PV},i} - P_{\mathrm{L},i} = U_i \sum_{j \in i} U_j \left(G_{ij}\cos\theta_{ij} + B_{ij}\sin\theta_{ij}\right), \quad i \in \{1, 2, \ldots, N\} \tag{11}$$

$$Q_{\mathrm{Sh},i} - Q_{\mathrm{L},i} = U_i \sum_{j \in i} U_j \left(G_{ij}\sin\theta_{ij} - B_{ij}\cos\theta_{ij}\right), \quad i \in \{1, 2, \ldots, N\} \tag{12}$$

$$\mathrm{Re}\left\{\boldsymbol{V}_{\mathrm{Sh}}(k)\boldsymbol{I}_{\mathrm{Sh}}(k)^*\right\} + \mathrm{Re}\left\{\boldsymbol{V}_{\mathrm{Se}}(k)\boldsymbol{I}_{\mathrm{Se}}(k)^*\right\} = 0, \quad k \in \{1, 2, \ldots, N_{\mathrm{U}}\} \tag{13}$$

$$\underline{U}_i \le U_i \le \overline{U}_i, \quad i \in \{1, 2, \ldots, N\} \tag{14}$$

$$S_{ij} \le \overline{S}_{ij}, \quad i, j \in \{1, 2, \ldots, N\} \tag{15}$$

$$0 \le \boldsymbol{S}_{\mathrm{Se}}(k) \le \overline{\boldsymbol{S}}_{\mathrm{Se}}(k) \le \overline{S}_{\mathrm{Se,max}}, \quad k \in \{1, 2, \ldots, N_{\mathrm{U}}\} \tag{16}$$

$$0 \le \boldsymbol{S}_{\mathrm{Sh}}(k) \le \overline{\boldsymbol{S}}_{\mathrm{Sh}}(k) \le \overline{S}_{\mathrm{Sh,max}}, \quad k \in \{1, 2, \ldots, N_{\mathrm{U}}\} \tag{17}$$

where f_{Cost} is the investment cost; the column vector $\boldsymbol{C}_{\mathrm{U}}$ is the construction cost per unit capacity of UPQC; λ_{U} is the ratio of annual operation and maintenance cost to construction cost; f_{Volt} is the voltage deviation; N_{U} is the number of UPQC; N_{B} is the number of branches; Scalars $\overline{S}_{\mathrm{Sh,max}}$ and $\overline{S}_{\mathrm{Se,max}}$ represent the upper limit of the allowable capacity of shunt and series parts of UPQC respectively; $U_{i,t}$ is the voltage of Node i in the tth period; N is the number of nodes; f_{Loss} is the line loss; Δt is the time step; T is the number of time intervals; R_j is the resistance of branch J; $I_{j,t}$ is the current of Branch j in the tth period, and N_{L} is the number of system branches; $P_{\mathrm{WG,i}}$ and $P_{\mathrm{PV,i}}$ are respectively the wind and photovoltaic power output of Node i; $P_{\mathrm{L,i}}$ and $Q_{\mathrm{L},i}$ are respectively the active load and reactive load of Node i; G_{ij} and B_{ij} are the conductance and susceptance between Node i and j; $j \in i$ indicates that Node j is directly connected with Node i; $\boldsymbol{V}_{\mathrm{Se}}(j)$ is the V_{Se} instruction value of the equivalent series controlled voltage source of the UPQC immediately adjacent to and upstream of Node j; $\overline{U}_i$ and $\underline{U}_i$ are respectively the upper and lower limits of U_i; S_{ij} is the apparent power of the line between Node i and j; $\overline{S}_{ij}$ is the power flow limit of

the line between Node i and j; The column vectors $\boldsymbol{S}_{\mathrm{Sh}}$ and $\boldsymbol{S}_{\mathrm{Se}}$ are respectively the apparent power of the shunt and series parts of UPQC.

4. Improved multi-objective golden eagle optimization algorithm

4.1. Introduction of golden eagle optimizer (GEO) algorithm

The core inspiration of GEO comes from golden eagles' strategy of adjusting flight speed at different stages of hunting spiral trajectories. When each Golden Eagle starts hunting, it will hover at a high altitude in its field and search for prey. The golden eagles share with each other the location of the best prey they have found so far. If it cannot find better prey, it will continue to turn around the current prey in a smaller circle and finally attack the prey. If it finds a better choice, it will fly around the new prey in a new circle and forget the previous prey. Each golden eagle randomly selects the best prey from the memory of other members of the eagle group and follows the one-to-one mapping strategy. They show more tendency to cruise and search for prey in the initial stage of hunting, and more tendency to attack in the final stage. By adjusting these two parts, the best prey in the feasible region can be captured in the shortest possible time.

Multi-objective golden eagle optimizer (MOGEO) is built on the basis of GEO, and then three additional concepts are introduced: (1) External archive: Competitive non-dominated solutions are saved in external archives, and with the optimization algorithm to update. Eagles are directed to archive members and ultimately to the Pareto front. (2) Prey priority criterion: The crowding distance of a solution on the Pareto front is defined as the distance between the two nearest solutions in its vicinity. In the non-dominated solution set, the non-inferior solution with a larger crowding distance will be more dominant. (3) Multi-objective prey selection: A roulette wheel-based prey selection process is adopted, where the weight is the inverse of the crowding distance of the current archived solution. This results in a higher probability of selection for solutions in sparse regions and a lower probability of selection for archive members in dense regions.

4.2. Improvement of MOGEO: Based on the two-archive strategy:

The archive in the MOGEO stores the set of historical elite solutions. In the next iteration, the solutions in the elite set are selected as the hunting targets of the golden eagle population, and are gradually approached. The advantage of this strategy is that the eagle group can quickly approach the elite solutions, so it has a higher convergence rate. However, the algorithm tends to fall into local optimums in the late iteration, resulting in the loss of population diversity.

In order to enhance the population diversity of the MOGEO algorithm, this paper introduces a two-archive strategy [7]. The one is the convergence archive (CA), which is used to store non-dominated solutions. The other is the diversity archive (DA), which stores both non-dominated and dominated solutions.

Assuming that N_{obj} is the number of objective functions of the optimization problem, the objective function corresponding to any solution in the archives can be expressed as

$$\boldsymbol{f} = [f_1, f_2, \ldots, f_{N_{\mathrm{obj}}}]^{\mathrm{T}} \tag{18}$$

The following definitions are proposed for $\boldsymbol{f}$.

(a) Crowding Coefficient

The density of the solutions set distributed in the vicinity of $\boldsymbol{f}$ is described by the Crowding Coefficient, that is,

$$CC(\boldsymbol{f}) = \begin{cases} 1 - \dfrac{1}{N_{\mathrm{obj}}} \displaystyle\sum_{j=1}^{N_{\mathrm{obj}}} \dfrac{f_{i+1,j} - f_{i,j}}{f_j^{\max} - f_j^{\min}}, i = 1 \\ 1 - \dfrac{1}{N_{\mathrm{obj}}} \displaystyle\sum_{j=1}^{N_{\mathrm{obj}}} \dfrac{f_{i+1,j} - f_{i-1,j}}{f_j^{\max} - f_j^{\min}}, i \in \{2, 3, \ldots, N-1\} \\ 1 - \dfrac{1}{N_{\mathrm{obj}}} \displaystyle\sum_{j=1}^{N_{\mathrm{obj}}} \dfrac{f_{i,j} - f_{i-1,j}}{f_j^{\max} - f_j^{\min}}, i = N \end{cases} \tag{19}$$

where N is the number of solutions in the current solution set; $f_{i,j}$ indicates that the value of the j-dimensional objective function of $\boldsymbol{f}$ is in the ith position from small to large in the current solution set.

(b) Dominated Index

The Dominated Index of $\boldsymbol{f}$ is defined as

$$DI(\boldsymbol{f}) = \frac{k}{n}, \quad \boldsymbol{f} \in P_k, \quad k \in \{1, 2, \ldots, n\} \tag{20}$$

$$P = P_1 \cup P_2 \cup \cdots \cup P_n \tag{21}$$

$$\boldsymbol{f}^1 \prec \boldsymbol{f}^2 \prec \ldots \prec \boldsymbol{f}^n, \quad \forall \boldsymbol{f}^j \in P_j, \quad j \in \{1, 2, \ldots, n\} \tag{22}$$

where P is the set of solutions in the archive; P_1, P_2, …, P_n are the subsets formed by non-dominated sorting of P from high to low according to the dominance level; $\boldsymbol{f}^i \prec \boldsymbol{f}^j$ means $\boldsymbol{f}^i$ dominates $\boldsymbol{f}^j$.

(c) Knockout Factor

Combining the Crowding Coefficient and Dominated Index, the Knockout Factor is defined as

$$KF(\boldsymbol{f}) = CC(\boldsymbol{f}) \times DI(\boldsymbol{f}) \tag{23}$$

From the above definitions, it is easy to conclude that the solution with a larger Knockout Factor will be regarded as the worse solution. Based on the above definitions, the pseudo-codes of the CA and DA update process are given below. In the proposed two-archive strategy, CA is used to push the population to the feasible region and approach the Pareto front; DA, as a supplement, is responsible for exploring areas under-exploited by the CA. It is worth noting that this paper selects the prey target from DA, rather than CA, for the next iteration of the golden eagle population. This improvement can make the optimization algorithm effectively enhance the diversity of solution set on the basis of ensuring convergence.

Algorithm 1: Pseudo-code of Update Mechanism of CA

```
Number of solutions in current CA: N=|CA|
P = current golden eagle population
for each X_i in P
    if X_i dominates one or more solutions {X_d} in the current CA then
        Remove {X_d} from CA, and add X_i to CA
    else if X_i is non-dominated to any solution in the current CA then
        if N < Maximum size of CA then
            Add X_i to CA
        else
            Calculate the Crowding Index for each solution within CA
            Select the outgoing CA solution using a roulette wheel weighted by Crowding Coefficient
            Replace the outgoing solution with X_i
        end
    end
end
Use nondominated sorting to divide P intoP_1, P_2, ..., P_n
Reserve ONLY P_1 in CA, and remove P_2, P_3, ..., P_n from CA
```

Algorithm 2: Pseudo-code of Update Mechanism of DA

```
Number of solutions in current DA: N=|DA|
P = current golden eagle population
for each X_i in P
    if N < Maximum size of DA then
        Add X_i to DA
    else
        Calculate the Knockout Factor for each solution in DA
        Select the outgoing DA solution using a roulette wheel weighted by Knockout Factor
        Replace the outgoing solution with X_i
    end
end
```

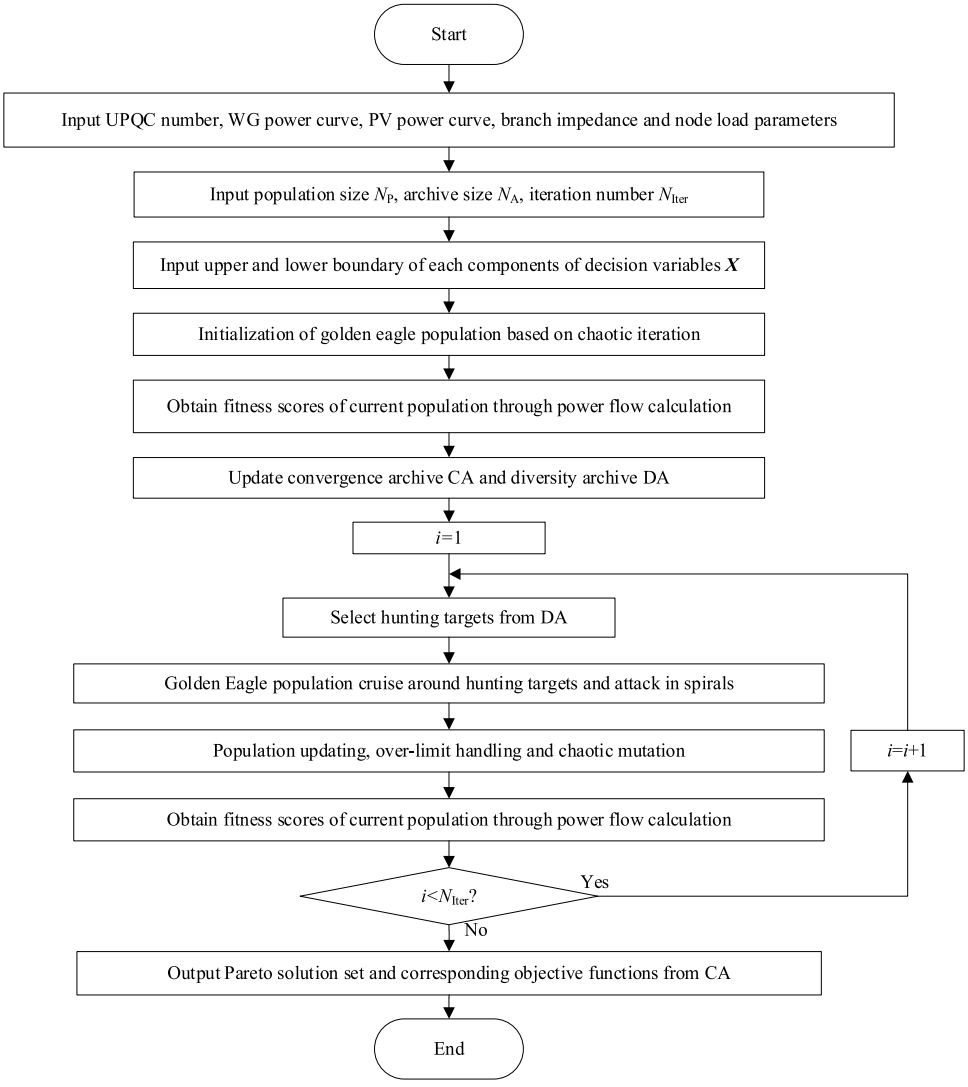

Fig. 3. The overall flow of the IMOGEO algorithm.

4.3. Overall process of the improved MOGEO

The overall flow of the improved multi-objective golden eagle optimization (IMOGEO) algorithm for optimal planning and dispatching of UPQCs is shown in Fig. 3.

5. Case study and optimization results

5.1. Study settings

The modified IEEE 33-node distribution grid model, as in Fig. 4, is used to verify the proposed optimization strategy for UPQC planning and dispatching. In this model, Node 0 is the substation node. Each branch is numbered the same as its right node, that is, the node at the receiving terminal. The network reference voltage is 10 kV. The total load of all nodes is 4.075MW +j 2.49MVar.

In the network, 6 distributed generators (DGs), i.e., 3 wind generators (WGs) and 3 photovoltaic power plants (PVs), are located on different nodes. The rated capacity of the 6 DGs is the same, 150 kVA. Among them, the

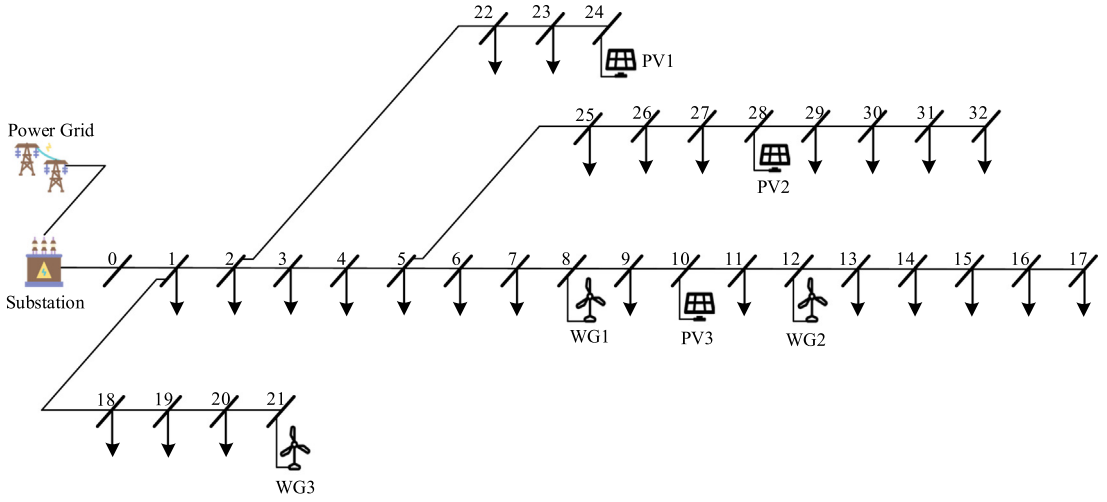

Fig. 4. Single-line diagram of the modified IEEE 33-node distribution grid.

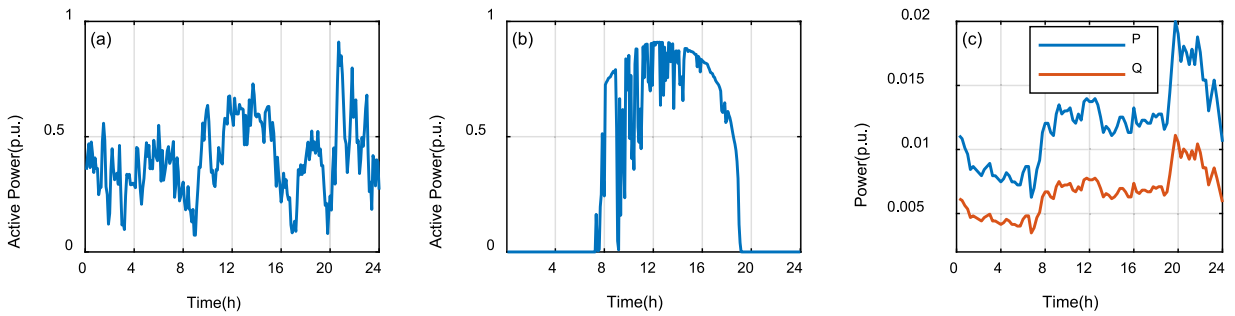

Fig. 5. Some examples of input data: (a) Output curve of WGs; (b) Output curve of PVs; (c) Daily load curve at Node 17. The base value is 150 kVA in (a) and (b), and 4.776 MVA in (c).

wind speed of 3 WGs and the light intensity of 3 PVs are modified from the NREL database [8,9]. For simplicity of problem formulation, it is assumed that all WGs have the same power output, and as do all PVs, as shown in Fig. 5. All DGs are assumed, for simplicity, with unity power factor.

The data of active and reactive load power are modified from a sparse distribution grid in Qinghai Province, China. Different load distributions are set for different nodes. Fig. 5(c) shows the daily load curve for Node 17 as an example.

The population size in the IMOGEO algorithm is 50, the archive capacity is 50, and the number of iterations is 1000. The node voltage range is set as 0.95∼1.05pu. The maximum allowable capacity of the parallel part and the series part of the UPQC is set to 0.6 MVA. The UPQC price is USD 1000/kVA. Operating costs account for 5% of investment costs. The convergence tolerance of the power flow calculation is set to $\varepsilon = 10^{-5}$.

5.2. Optimization results

The optimization results using the IMOGEO algorithm are shown in Fig. 6. Several representative solutions are marked in the optimal solution set in Fig. 6. The fitting surface in the figure schematically shows the Pareto front. Based on the optimal solution set, the relationship between each objective function can be better revealed. The optimal solutions under different target values are given, and a variety of options are provided for decision makers.

Table 1 shows the corresponding UPQC location and capacity scheme of the 4 marked solutions mentioned above, as well as the corresponding voltage deviation, line loss, and cost. The condition without UPQC installed is also carried out as a comparison. In Table 1, Solution 1 has the smallest voltage deviation, Solution 2 has the

Table 1. Typical optimized schemes of location and capacity of UPQCs.

Solution Mark	Location and capacity of UPQCs (Branch number (kVA))	Voltage deviation /kV	Line loss /MW	Cost /US$ million
0	No UPQC installed	0.660	0.160	0
1	2(1548), 5(667), 27(472), 9(660)	0.120	0.155	3.52
2	2(760), 12(887), 19(1140), 26(1131)	0.207	0.138	4.12
3	5(534), 9(192), 21(140), 29(256)	0.190	0.154	1.18
4	4(512), 10(431), 23(213), 27(206)	0.147	0.146	1.43

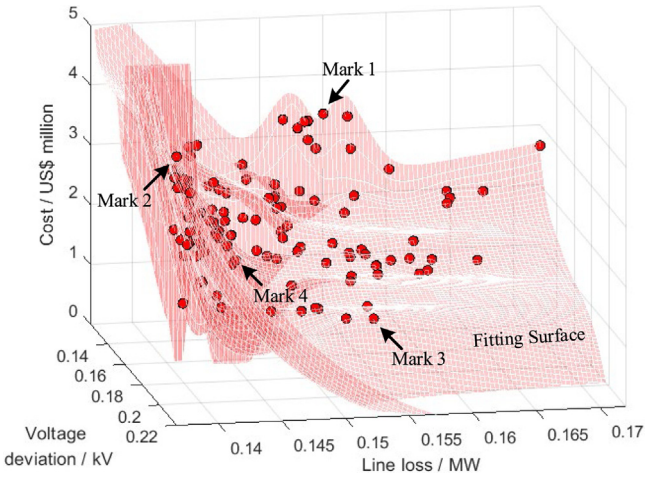

Fig. 6. The optimal solution set obtained by the proposed IMOGEO algorithm.

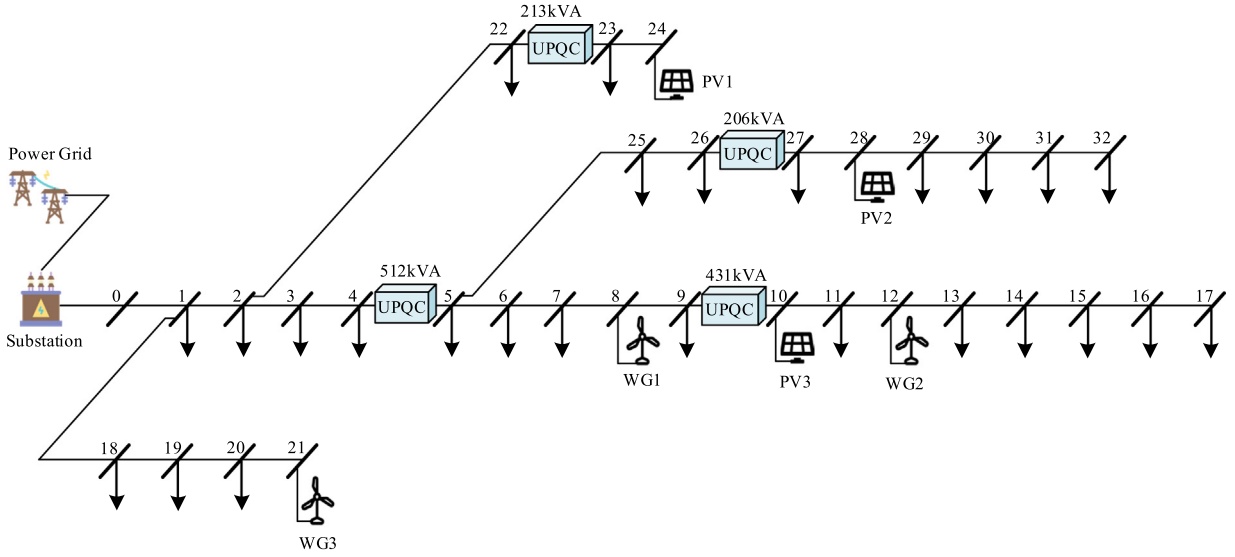

Fig. 7. Schematic diagram of an optimized scheme of location and capacity of UPQCs.

smallest line loss, Solution 3 has the lowest cost, and Solution 4 is a compromise scheme. Fig. 7 shows the UPQC location and capacity configuration scheme of scheme 4.

In addition to the optimized planning scheme, the optimized dispatching instructions required for the operation of UPQCs are also obtained. Here, the dispatching strategy matching Solution 4 is selected as an example. The voltage data of each node at each moment are obtained through simulation. To reveal the superiority of this dispatching

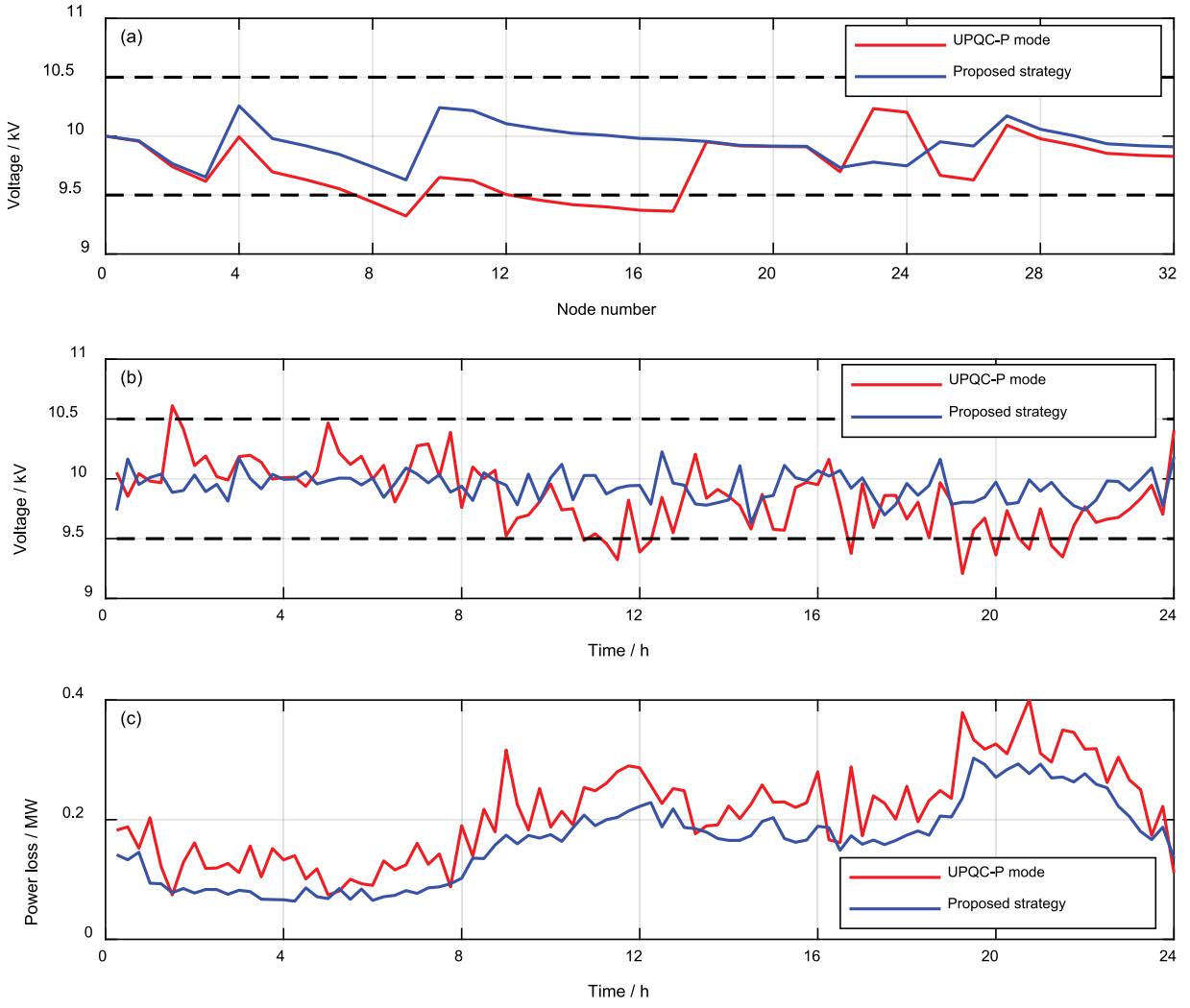

Fig. 8. Performance comparison of two dispatching strategies illustrated by typical examples: (a) Voltage profile at 20:00; (b) Diurnal voltage variation at Node 17; (c) Diurnal variation of line loss.

strategy, the simulation results under UPQC-P mode are used as a comparison, as shown in Fig. 8. The voltage profile at 20:00 and the voltage diurnal variation at Node 17, as examples, are respectively plotted in Fig. 8(a) and (b). Under the proposed dispatching strategy, the voltage fluctuation can be kept within a limited range. Fig. 8(c) shows the diurnal variation of line loss under the two operation modes, comparatively. It can be seen that the dispatching strategy proposed in this paper can effectively reduce line loss. Therefore, compared with the UPQC-P mode, the optimized dispatching strategy proposed in this paper has better performance in minimizing voltage deviation and line loss.

6. Conclusion

With the large-scale integration of renewable energy, the use of UPQC is increasing for power quality management and reactive power compensation in distribution grids. An optimization method for location and capacity planning of UPQCs is proposed for the distribution grid with distributed generators. The planning and dispatching of UPQCs are combined into a coupled optimization model in this paper. The dual-controlled-source model is proposed and well used to describe the operation state of UPQC. Fluctuations in the output of wind generators and photovoltaic power plants are also taken into account. The proposed IMOGEO algorithm, containing

the two-archive strategy, can better balance the convergence and diversity of the non-dominated solution set. A case study is carried out based on the modified IEEE 33-node distribution grid model including DGs and loads with a diurnal variation. The optimized schemes of location and capacity planning are obtained, and the corresponding dispatching strategies display the superiority in both voltage variation and line loss. The results verify the effectiveness and advantages of the proposed method. This method has guiding and promoting significance for green energy integration and power quality management of distribution grids. Moreover, other intelligent algorithms as well as optimization models for this problem will be discussed in the further research.

Declaration of competing interest

The authors declare that they have no known competing financial interests or personal relationships that could have appeared to influence the work reported in this paper.

Data availability

Data will be made available on request.

Acknowledgments

This work is supported by State Grid Qinghai Electric Power Company Project, China (5228201900G5).

References

[1] Yang RH, Jin JX. Unified power quality conditioner with advanced dual control for performance improvement of DFIG-based wind farm. IEEE Trans Sustain Energy 2021;12:116–26.
[2] Ganguly S. Multi-objective planning for reactive power compensation of radial distribution networks with unified power quality conditioner allocation using particle swarm optimization. IEEE Trans Power Syst 2014;29:1801–10.
[3] Sarker J, Goswami SK. Optimal location of unified power quality conditioner in distribution system for power quality improvement. Int J Electr Power Energy Syst 2016;83:309–24.
[4] Han J, Li X, Sun Y, Luo D, Huang S. Optimal operation of UPQC under VA capacity constraints based on hierarchical optimization. Int J Electr Power Energy Syst 2020;122:106168.
[5] Amini M, Jalilian A. Optimal sizing and location of open-UPQC in distribution networks considering load growth. Int J Electr Power Energy Syst 2021;130.
[6] Mohammadi-Balani A, Dehghan Nayeri M, Azar A, Taghizadeh-Yazdi M. Golden eagle optimizer: A nature-inspired metaheuristic algorithm. Comput Ind Eng 2021;152:107050.
[7] Li K, Chen R, Fu G, Yao X. Two-archive evolutionary algorithm for constrained multiobjective optimization. IEEE Trans Evol Comput 2019;23:303–15.
[8] Jager D, Andreas A. NREL national wind technology center (NWTC): M2 tower, Boulder, Colorado (Data). NREL report No. DA-5500-56489, 1996, http://dx.doi.org/10.5439/1052222.
[9] Sengupta M, Andreas A. Oahu solar measurement grid (1-year archive): 1-Second solar irradiance, Oahu, Hawaii (Data). NREL report No. DA-5500-56506, 2010, http://dx.doi.org/10.5439/1052451.